Exploring Origins of Interfacial Yielding and Wall Slip in Entangled Linear Melts during Shear or after Shear Cessation

Pouyan E. Boukany and Shi-Qing Wang*

Department of Polymer Science and Maurice Morton Institute of Polymer Science, University of Akron, Akron, Ohio 44325

Received November 25, 2008; Revised Manuscript Received January 24, 2009

ABSTRACT: We study yielding at interface between a solid wall and entangled polymer melts. At a average rate higher than the terminal relaxation rate, a combination of rheometric and particle-tracking velocimetric (PTV) measurements reveals apparent wall slip (or interfacial yielding) at a strain γ_{iy}, just beyond the stress overshoot. PTV observations show that the interfacial yielding occurs at a higher strain in the presence of a faster rate of shear. Shear cessation at a strain lower than γ_{iy} is observed to also result in interfacial failure, suggesting that the finite adhesion can be overcome in quiescence by the residual elastic retraction force. These two kinds of interfacial failure can be theoretically understood in terms of the intrachain elastic retraction forces overcoming the melt adhesion arising from interchain entanglement interactions between adsorbed and bulk chains.

I. Introduction

Significant wall slip can occur in well-entangled polymers in simple shear. In 1979, de Gennes first explained why massive wall slip is possible for entangled polymers.[1] Since then, various theoretical studies[2−6] have been carried out to describe how the Navier−de Gennes extrapolation length b depends on the flow condition such as the shear stress or the imposed velocity. These publications explored the consequences of having different values of a slip velocity V_s at the polymer/wall interface by assuming that it preexists at the interface. They concentrated on describing how the magnitude of slip depends on either shear stress or shear rate in steady state instead of depicting how and when wall slip arises during sudden startup shear. Moreover, there has not been any discussion about what deformation condition would result in bulk failure instead of interfacial breakdown. Only in the limit of low surface coverage could they explain how interfacial disentanglement arises when the tethered chains are exposed to sufficiently high V_s.

Since the state of chain adsorption for a given pair of polymer and wall is challenging to predict, realistic theoretical modeling has been difficult to formulate. If sufficient chain adsorption is present, V_s must initially be zero upon startup shear. Only in the limit of mushroom coverage did Brochard and de Gennes find[2] the maximum wall slip to occur when the tethered chains undergo coil−stretch transition to become disentangled from the unbound bulk chains. This picture leaves us with an impression that coil-to-stretch is the route to disentanglement and wall slip. Mhetar and Archer suggested[5] that the critical force for a tethered chain to disentangle from the bulk chains grows linearly with the chain length, whereas the French workers[2−4] arrived at a critical stress independent of chain length. Lele and Joshi attempted[7,8] to treat wall slip in steady shear without prescribing a finite preexisting V_s at the interface. Experiments involving natural physical adsorption have revealed[9−11] a critical shear stress for an interfacial stick−slip transition that is independent of the polymer molecular weight.

Over the past two decades, wall slip in polymer melts and solutions has been a constant experimental theme and extensively studied using a variety of setups and methods.[12−20] Despite increasing knowledge on the topic of polymer wall slip,[21] there is no theoretical understanding to address the following interesting questions in case of strong polymer adsorption: (1) How does wall slip first emerge during a startup shear? (2) Is wall slip the only mechanism of material failure? (3) Could interfacial failure take place after shear cessation? Recent activities based on particle-tracking velocimetric observations (PTV)[22] have allowed us to correlate conventional rheological measurements with the corresponding deformation field. Specifically, the combination of PTV and rheological methods has helped us to propose a different set of theoretical considerations.[23] For example, we have come to appreciate that entangled polymeric liquids possess a level of cohesion on short time scales that can be universally quantified in terms of their elastic plateau modulus. Consequently, entangled liquids actually yield during rapid continual deformation.[23,24] The PTV observations enabled us to determine whether the yielding could occur homogeneously or amount to localized failure of the chain entanglement network.

In the present work, we show that for well entangled melts the stress overshoot upon startup shear is correlated with interfacial yielding or apparent wall slip at melt/wall interfaces. This interfacial failure first occurs upon reaching strain γ_{iy}. On the other hand, the same sample such as the present polyisoprene (PI) melts is observed to undergo interfacial yielding in quiescence when the startup shear is terminated at strains lower than γ_{iy}. This "arrested" interfacial failure phenomenon is difficult to explain according to any available theoretical depiction of wall slip. Such phenomenon is expected from the emerging theoretical picture[23] that is modified here for the interface. The observations of interfacial failures either during or after shear offer an explicit explanation of why the relaxation process, as quantified conventionally by the damping function h, exhibits severe strain softening.

II. Experimental Section

A. Materials. This study focuses on interfacial behavior of monodisperse polyisoprene melts. Two relatively monodisperse PI melts (labeled as PI300K and PI550K) were provided to us by Goodyear via courtesy of Dr. Adel Halasa. They have similar microstructures: *cis*-1,4 (75.2%), *trans*-1,4 (17.8%), and −3.4 (7.0%) for PI300K and *cis*-1,4 (75.0%), *trans*-1,4 (16.4%), and −3.4 (6.6%) for PI550K. Their other molecular characteristics are listed in Table 1. About 600 ppm of silver-coated particles of average 10 μm size was solution-mixed with the PI melts to allow PTV observations during and after startup shear. The solvent (toluene) is subsequently removed in the hood and vacuum oven. With a

* Corresponding author: e-mail swang@uakron.edu.

10.1021/ma802644r CCC: $40.75
Published on Web 02/23/2009

Table 1. Molecular Characteristics of PI300K and PI550K

sample	M_n (g/mol)	M_w (g/mol)	M_w/M_n	τ (s)	b_{max} (mm)	$V_{s(max)}$ (mm s^{-1})	$(Wi)_c$
PI300K	291K	311K	1.07	4.9	0.8	0.16	3[a]
PI550K	516K	547K	1.06	50	11	0.22	29[a]

[a] Calculated according to $(Wi)_c = (1 + 2b_{max}/H)$ by taking $H = 0.8$ mm.

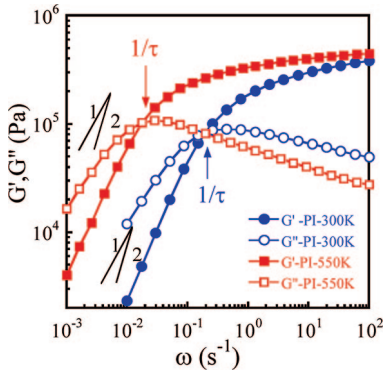

Figure 1. Small-amplitude oscillatory measurements of storage and loss moduli G' and G'' for PI330K and PI550K melts, where the scaling behavior in the terminal regime deviates from those scaling laws expected of more monodisperse melts. Thus, the crossover frequency could only approximately represent the reciprocal terminal relaxation time, τ^{-1}.

CRAVER press, bubble-free sheets of the PI samples can be prepared for loading onto a sliding plate rheometer.

B. Apparatuses. A dynamic mechanical spectrometer (Advanced Rheometric Expansion System-ARES) was used to obtain storage and loss moduli G' and G'' at frequencies ranging from 0.001 to 100 rad/s at room temperature in 25 mm parallel-plate geometry. Figure 1 shows the two sets of data for each of the two PI melts. The terminal relaxation time τ is listed in Table 1 along with other important characteristic parameters to be discussed in the text.

A custom-made sliding-plate shear rheometer was employed in the present study. With the bottom plate fixed, the movable upper plate is displaced by a step motor (Motion Parker Co, model ZETA6104-57-83), where the resulting force is measured by a load cell (Honeywell Co., model 13)[25] that has measurement range from 1.5 to 450 N. The velocity of the upper plate can be read from the program controlling the step motor. More details about this rheometer have been given elsewhere.[25]

Typically, a sample of 35 mm by 10 mm and thickness H around 0.7−0.9 mm is placed on the lower plate. After the top plate is installed, the sample was allowed to establish sufficient adsorption on both plates overnight. The particle-tracking velocimetric (PTV) setup for this sliding plate rheometer has been described previously.[25] For the purpose of PTV measurements, both plates are black-painted by a thin layer of black enamel (Rustoleum Corp., specialty high heat black enamel) to minimize reflection, where a small window was made on the lower stationary plate to allow laser illumination. All the measurements were carried out at room temperature around 24 °C.

III. Characterization of Wall Slip and Theoretical Picture of Interfacial Yielding

A. Phenomenological Depiction of Wall Slip and Its Upper Bound. A simple phenomenological depiction of wall slip has been around for 30 years ever since the pioneering paper of de Gennes[1] that rediscovered the notion of slip length first introduced by Navier. In terms of a interfacial friction coefficient $\beta = \eta_i/a$, de Gennes proposed that the slip velocity V_s be related to the shear stress σ as

$$V_s = \sigma/\beta = \sigma a/\eta_i \quad (1)$$

where η_i is a local viscosity at the interface and a is an interfacial thickness. Note that this definition of eq 1 does not prescribe how η_i may depend on σ. In the case of a sudden startup shear with imposed mean rate $\dot{\gamma}$, neither V_s nor σ is an experimentally controlled parameter. In steady-state simple shear between two parallel plates of separation H at $\dot{\gamma} = V/H$, if wall slip is present on both interfaces with slip velocity V_s, the actual bulk shear rate in $\dot{\gamma}_{tru} = V_b/H$ that produces $\sigma = \eta\dot{\gamma}_{tru}$ is lower than $\dot{\gamma}$ according to

$$\dot{\gamma}_{tru} = \dot{\gamma}/(1 + 2b/H) \quad (2)$$

because $V = V_b + 2V_s$. Here the Navier−de Gennes extrapolation (slip) length[1] $b = \eta/\beta$ has its direct meaning of "extrapolation" through its definition[11] of $V_s = b\dot{\gamma}_{tru}$ and η is the shear viscosity of the bulk sample. Interfacial slip occurs when the sample is sheared beyond the terminal flow regime, i.e., when $\dot{\gamma}\tau > 1$. The maximum amount of wall slip occurs when chain disentanglement reduces η_i to η_e (i.e., the viscosity of a Rouse melt of entanglement molecular weight M_e) during stick−slip transition (SST) at a critical shear stress.[11] At this SST, a in eq 1 equals the entanglement spacing l_{ent} while the bulk still undergoes terminal flow at a shear stress level comparable to the plateau modulus G_N^0. Under this condition, the bulk shear rate is $\dot{\gamma}_{tru} = \sigma/\eta_0 \sim G_N^0/\eta_0 \sim 1/\tau$, where use is made of $\eta_0 \sim G_N^0\tau$, relating the zero-shear viscosity η_0 to the quiescent terminal relaxation time τ. The upper bound for b is given by[11,21]

$$b_{max} = (\eta_0/\eta_e)l_{ent} = (\tau/\tau_e)l_{ent} \quad (3)$$

where the second equality follows from $\eta_e \sim G_N^0\tau_e$, with τ_e being the tube constraint time in the tube model.[26] Table 1 lists the measured values of b_{max} from a previous study,[11] where the value for PI550K is obtained from that for PI300K by a multiplicative factor of the zero-shear viscosity ratio η_0(PI550K)/η_0(PI300K) obtained from Figure 1. The corresponding maximum slip velocity V_s is given by[11,21]

$$V_{s(max)} = b_{max}\dot{\gamma}_{tru} \sim b_{max}/\tau = l_{ent}/\tau_e \quad (4)$$

where eq 3 was used to express b_{max}. Equation 4 shows a molecular-weight-independent quantity, depicting the speed of movements free of chain entanglement. In other words, eq 4 indicates how the microscopic dynamics at the length scale of entanglement spacing determine the upper bound for interfacial slip velocity upon chain disentanglement. Actually, $V_{s(max)}/l_{ent} \sim 1/\tau_e$ is the magnitude of the shear rate that exists in the entanglement-free interfacial layer upon the SST. This formula also suggests that τ_e at room temperature can be directly obtained through the room-temperature measurement of the maximum slip velocity as carried out previously[11] without resort to linear viscoelastic measurements, the time−temperature superposition principle and WLF relationship. From the published value of $l_{ent} \sim 6$ nm for the 1,4-PI melt[27] and the experimentally determined $V_{s(max)} \sim 0.22$ mm/s for PI550K, we obtain $\tau_e \sim 2.7 \times 10^{-5}$ s from eq 4, which is consistent in magnitude with an estimate according to an empirical formula $\tau/\tau_e \sim (M_w/M_e)^{3.3}$ that gives $\tau_e \sim 1.7 \times 10^{-5}$ s, taking $\tau = 50$ s from Table 1, $M_w = 550$ kg/mol, and $M_e = 6$ kg/mol for the 1,4-PI melt.[27] Similarly, for 1,4-polybutadiene melts, with $V_{s(max)} \sim 23$ mm/s according to ref 11 and $l_{ent} \sim 4.6$ nm,[27] eq 4 gives $\tau_e \sim 2 \times 10^{-7}$ s, in agreement with a previous direct rheological measurements,[28] which successfully applied the WLF time−temperature superposition principle to explore the full relaxation spectrum from τ to τ_e. Moreover, if the temperature dependence of τ_e would be different from that of the terminal relaxation time τ, one can in principle measure the temperature dependence of $V_{s(max)}$ to confirm. This exercise of estimating τ_e from the maximum slip velocity $V_{s(max)}$ given in eq 4 underscores the power of the theoretical description of wall slip given in eqs

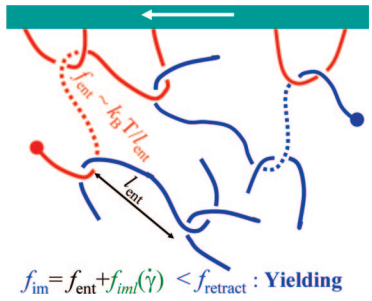

Figure 2. Depiction of entanglement interactions between some adsorbed (red) chains and free bulk (blue) chains, where adhesion (i.e., interfacial cohesion) exists between the two different kinds of chains. According to refs 23 and 24, there is k_BT of conformational entropy associated with each strand between entanglement, amounting to a cohesive (entanglement) force f_{ent} of magnitude comparable to k_BT/l_{ent}, where l_{ent} is mean end-to-end distance of the strand between entanglements. The total intermolecular force f_{im} is a summation of the quiescent cohesion force f_{ent} and the intermolecular locking force f_{iml} that vanishes upon shear cessation. Imposition of sudden startup shear may cause the entanglement strands at the chain ends to first disengage, either during shear beyond the yield point when $f_{retract} > f_{im}$ in magnitude to allow interchain sliding or after shear cessation when f_{im} instantly reduces to f_{ent} and the residual elastic restoring force $f_{retract} > f_{ent}$.

1−4. In passing, note that the slip length b is a more suitable parameter to quantify wall slip either when comparison is needed between different polymers or at different temperatures[21] because b is an inherent parameter, dependent only on the entanglement characteristics but independent of temperature, whereas the magnitude of V_s changes with temperature as the relaxation time does.

B. Interfacial Yielding during and after Shear. The preceding phenomenological quantification of wall slip avoided the more interesting question of why and how wall slip arises upon shear deformation. Wall slip, as a natural experimental complication, prevents us from testing theories for bulk polymer dynamics such as the Doi−Edwards tube theory in the nonlinear response regime. It should be clear from the onset that for strongly adsorbing surfaces wall slip does not occur in the terminal flow (linear response) regime where chain disengagement occurs on its own natural time scale of reptation, and entanglement network is therefore not forced to disintegrate.

For well-entangled polymer melts and solutions, sudden deformation can be made rapidly in a rheometric test relative to the terminal relaxation time τ. A shear strain higher than unity can occur within a time shorter than τ when the Weissenberg number $Wi = \dot{\gamma}\tau > 1$. In our picture[24] modified here to bring the polymer/wall interface into discussion as shown in Figure 2, deformation of any given test chain is due to intermolecular locking force f_{iml}. At a high rate $\dot{\gamma}$ (i.e., $Wi > 1$), a yield point will be reached when the intrachain elastic retraction force $f_{retract}$ grows with γ to be as high as the declining intermolecular gripping force f_{iml} at the shear stress maximum.[24] Beyond this point denoted by the elapsed strain γ_{iy} (where the subscript stands for interfacial yielding), the shear stress declines as mutual sliding occurs between the adsorbed (red) chains and the surrounding unbound (blue) chains until entanglement escapes from the chain ends. In other words, load-bearing strands disappear as the red and blue chains move pass one another. The chain disentanglement can occur either to the red chain or to the blue chain as depicted in Figure 2 as the moving wall displaces toward the left-hand side, where the chain ends are decorated with dots. Re-entanglement cannot occur if sufficient shear is present to carry the free chains past the adsorbed chains, a condition that depends on the external condition. The present discussion only indicates how yielding could occur at the interface due to loss of entanglement strands as depicted in Figure 2 during continual shear. A more general picture has been suggested for bulk cohesive failure.[23,24] The system fails at the melt/wall interface instead of suffering internal failure at a low Weissenberg number because there are usually not as many entanglements at the interface as there are in the sample interior.

According to eq 2, the externally imposed apparent shear rate $\dot{\gamma}$ can be as high as $(1 + 2b_{max}/H)/\tau$ without forcing the bulk sample to go beyond the terminal flow regime whose upper bound is given by a shear rate of $1/\tau$, i.e., $Wi = 1$. In other words, when the Weissenberg number $Wi = \dot{\gamma}\tau$ is higher than $(Wi)_c = (1 + 2b_{max}/H)$, the bulk of the sample can no longer avoid undergoing shear beyond terminal flow. The interfacial yielding may now involve a layer thickness higher than the entanglement spacing $l_{ent} \sim 6$ nm. One purpose of the present study is to compare experiment with this theoretically predicted transformation from wall slip to interfacial yielding (bulk failure at the interface).

One only needs to perform a small-amplitude step strain to confirm that there actually exists finite adhesion due to the interfacial chain entanglement depicted in Figure 2. In other words, interfacial failure cannot occur at sufficiently small strains. The adhesion is associated with ca. 1 k_BT entropic energy in each strand between interfacial entanglements as shown in Figure 2. If an interfacial or bulk strand next to the chain end (denoted by the dashed lines) is to disengage from the network, it has to overcome an entanglement force $f_{ent} \sim k_BT/l_{ent}$ and temporarily suffer an entropy loss on the order of k_BT. In the case of small step strain with $\gamma_0 \ll 1$, the elastic retraction force ($f_{retract} \ll f_{ent}$) is insufficient to overcome the cohesion either at the interface or in the bulk, and consequently relaxation takes place quiescently.

The situation becomes interesting when a continual shear is interrupted at a large amplitude γ_0 but still lower than γ_{iy} that is the critical strain where interfacial yielding (apparent slip) is first observed during shear. According to a recent theoretical depiction,[23] a sudden large step strain with γ_0 can build sufficiently high elastic retraction force in each entanglement strand, i.e., produce $f_{retract} \sim \gamma f_{ent}$. Upon shear cessation, f_{iml} turns off instantly,[24] leaving the quiescent cohesion force

$$f_{ent} \sim k_BT/l_{ent} \tag{5}$$

alone to counterbalance the restoring force $f_{retract}$. The system can become unstable if $f_{retract} > f_{ent}$. In other words, even though no wall slip would occur during shear up to γ_{iy}, interfacial failure can take place upon shear cessation at $\gamma_0 < \gamma_{iy}$. A second goal of the present study is to explore whether such predicted behavior, which we call "arrested" interfacial failure (apparent slip), indeed occurs. Experimental confirmation of such a phenomenon would lend powerful support for the molecular picture[23,24] presented here and elsewhere.

IV. Results and Discussion

Although startup shear of entangled polymers is a commonly used protocol for interrogation of nonlinear rheological behavior, premature failure at the polymer/wall interface often prevents the prescribed deformation from being actually imposed. The effort to address this challenge and eliminate interfacial slip will be reported in the near future.[29] At the present, we focus on various aspects of interfacial phenomena including wall slip. Given a smooth flat solid surface, measurable wall slip is inevitable for well-entangled polymer melts at high rates and stresses. The present study will show using PTV observations that relatively monodisperse polyisoprene melts undergo interfacial yielding either during shear or after shear cessation.

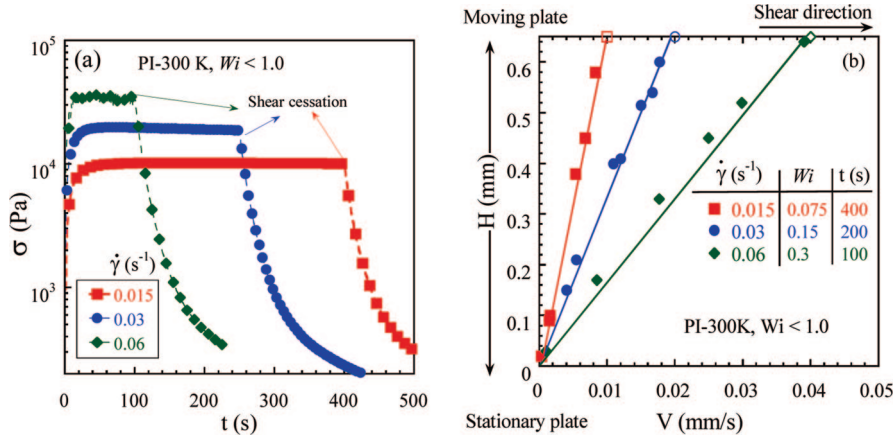

Figure 3. (a) Shear stress growth and relaxation in the terminal flow regime at three rates of 0.015, 0.03, and 0.06 s^{-1}. (b) PTV measurements revealing homogeneous shear at these three rates and absence of any interfacial slip.

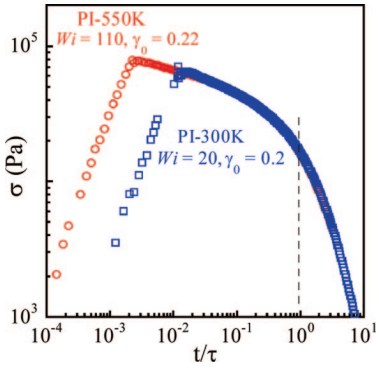

Figure 4. Shear stress growth and relaxation upon and after a small step strain of $\gamma_0 = 0.2$ for both PI melts, showing identical relaxation behavior on the normalized time scale of t/τ, where shear cessation occurs at $t_0/\tau = \gamma_0/\dot{\gamma}\tau = \gamma_0/Wi$, which explains the separation of a factor of 110/20 = 5.5 apart between the two points of shear cessation for PI300K and PI550K.

A. Linear Responses. As explained in the preceding section, wall slip is inevitable when an entangled polymer is sheared by displacement of one of the two parallel surfaces at a velocity V higher than $H\tau$, i.e., when Weissenberg number $Wi \geq 1$ and the imposed strain exceeds unity. In contrast, we ought to see homogeneous shear without slip for $Wi < 1$ and linear relaxation. Our experiments in terminal flow indeed confirm that the deformation takes place homogeneously without any visible interfacial failure as shown in Figure 3a,b based on the PI-300K melt. Moreover, upon shear cessation, the sample relaxes quiescently.

Step shear experiments at low amplitude are well-defined because of finite adhesion between a polymer melt and a flat smooth solid wall. In other words, these tests not only reveal linear response in terms of quiescent stress relaxation but also confirm existence of finite interfacial strength due to physical polymer adsorption. For well-entangled melts, such a stress relaxation experiment also suggests existence of chain entanglement. Figure 4 shows that upon truncation of a startup shear at $\gamma_0 \sim 0.2$ both PI melts relax identically on a normalized time scale, exhibiting initial elasticity until the terminal relaxation time τ at the vertical dashed line. At such a low strain, the relaxation occurs quiescently according to the PTV observations.

B. Interfacial Yielding during Shear. At higher shear rates $0.46 \geq \dot{\gamma} \geq 0.15$ s^{-1} ($2.3 \geq Wi \geq 0.75$), the deviation from linear velocity field with visible slip is observable from Figure 5a. The inset shows that the shear stress exhibits a maximum during the startup shear. The bulk shear rate $\dot{\gamma}_{tru}$ is around 0.18 s^{-1} (comparable to the reciprocal relaxation time, $\tau^{-1} \approx 0.2$ s^{-1}) at apparent shear rates of 0.3 and 0.46 s^{-1}. At 0.46 s^{-1}, corresponding to $Wi = 2.3$, which is close to the critical value $(Wi)_c = 1 + 2b_{max}/H \approx 3$, the slip velocity is around 0.13 mm/s, comparable to the maximum theoretical slip velocity of $V_{s(max)} = 0.16$ mm/s. These measurements are fully consistent with the theoretical description presented in section III. Our PTV method with a spatial resolution of ca. 20 μm cannot claim that the observed V_s is truly the slip velocity, involving wall slip instead of bulk failure. However, because the magnitude of V_s did not exceed the maximum value of slip velocity of 0.16 mm/s, the PTV observation is likely to have revealed nothing but true wall slip.

We further examine the wall slip behavior using the second sample of PI550K. Figure 5b reveals that at $Wi \sim 1.25$ the velocity profile initially is linear across the gap before the stress overshoot at $t \sim 50$ s. At $t = 60$ s, strong recoil-like failure occurs corresponding to the moment of sharp shear stress decline. At longer times, oscillation of the shear stress synchronizes with a stick−slip oscillation of the boundary condition. This stick−slip oscillation has been seen before in entangled polymer melts.[18,20]

At a higher Weissenberg number involving shear rate of 4 s^{-1} ($Wi = 20$) the PI300K melt undergoes uniform deformation until the elapsed strain reaches $\gamma_{iy} = 1.5$, beyond which, i.e., beyond $t_{iy} = 0.375$ s, interfacial failure is observed, and the shear stress starts to decline. In this experiment illustrated in Figure 6a, the displacement of the upper plate is stopped at $t_0 = 0.5$ s. A similar startup shear is carried out all the way to a strain of $\gamma_0 = 8.8$ for PI550K as shown in the same figure, where the stress maximum occurs at $\gamma_{iy} = 2.0$ for $Wi = 110$. In addition, in situ PTV observations were carried out to track the deformation fields over time during and after shear as shown in Figure 6b,c for both PI300K and PI550K, respectively. Interfacial failure showed up beyond $\gamma_{iy} = 1.5$ for PI300K and $\gamma_{iy} = 2.0$ for PI550K with interfacial velocity $V_i > 1$ mm/s, which considerably higher than the maximum slip velocity $V_{s(max)}$ tabulated in Table 1. This suggests that the sample has actually suffered yielding that is not limited to the interface but has spread into the sample interior. Although the present PTV technique cannot resolve it, the entanglement-free interfacial layer must be greater in thickness than the entanglement spacing of 6 nm. Conceptually, we have presumably observed interfacial yielding that has extended into the sample bulk and is not strictly wall slip.

The PTV observations also offer an explicit account for the sharp shear stress decline at the end of the shear cessation at $\gamma_0 = 2.0$ and 8.8 respectively for PI300K and PI550K melts. The

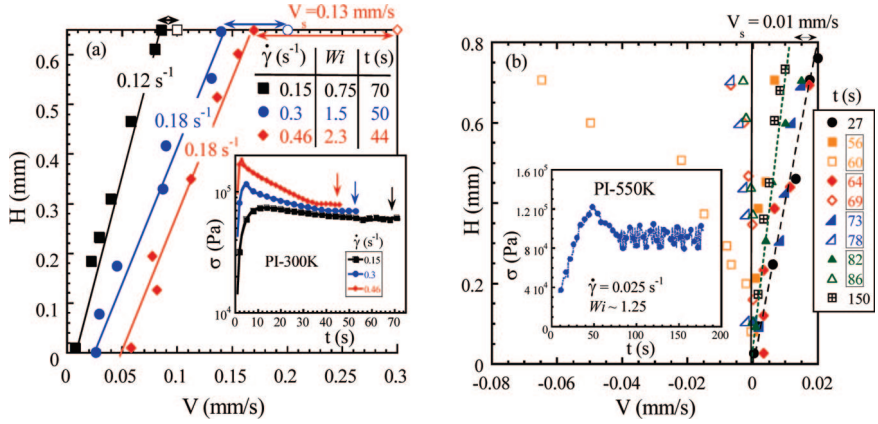

Figure 5. (a) PTV observations of wall slip beyond the terminal flow regime for PI300K melt at three applied rates of 0.15, 0.3, and 0.46 s^{-1}, where the open symbols denote the prescribed top plate velocities and slip velocity V_s are also indicated for each rate. The true shear rates in the bulk are only 0.12, 0.18, and 0.18 s^{-1}, respectively, as indicated. The inset shows the stress overshoot characteristics at each rate, where the vertical arrows indicate the moments when the PTV measurements were made. (b) At a Weissenberg number $Wi = 1.25$ just beyond the terminal flow regime, the PTV shows stick−slip oscillation for the PI550K melt, where the data are grouped into pairs of two distinct moments in each oscillation cycle and the open squares show the initial maximum recoil-like motion. The inset shows the corresponding oscillatory shear stress as a function of time.

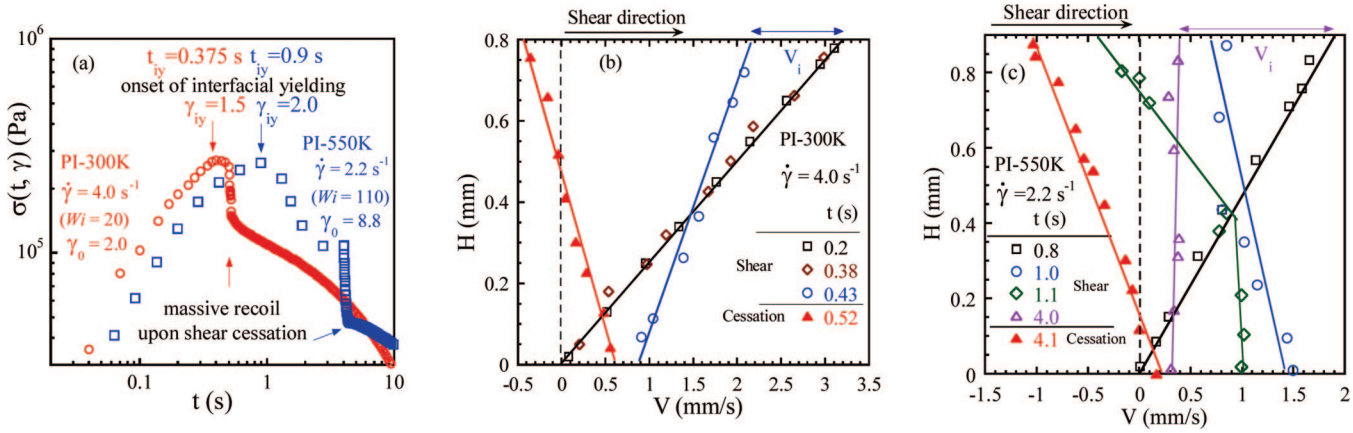

Figure 6. (a) Shear stress growth and relaxation upon termination of a startup shear at $\gamma_0 = 2.0$ for PI300K melt (circles) involving $Wi = 20$, where interfacial yielding was first detected by PTV when $\dot{\gamma}t_{iy} = \gamma_{iy} = 1.5$. A much higher $Wi = 110$ was applied for 8.8 strain units before shear cessation for PI550K melt (squares) that shows the first sign of interfacial yielding at $\gamma_{iy} = 2.0$. PTV observations reveal interfacial failure during shear and recoil-like motions after shear cessation for (b) PI300K and (c) PI550K melts, respectively. The squares at $t = 0.2$ in (b) and $t = 0.8$ in (c) indicate the initial homogeneous deformation. The other open symbols in (b) and (c) denote the velocity field at other times during shear. The filled triangles show how the samples recoil due to massive interfacial failure on the top plate 0.2 and 0.1 s, respectively, after shear cessation in PI300K and PI550K.

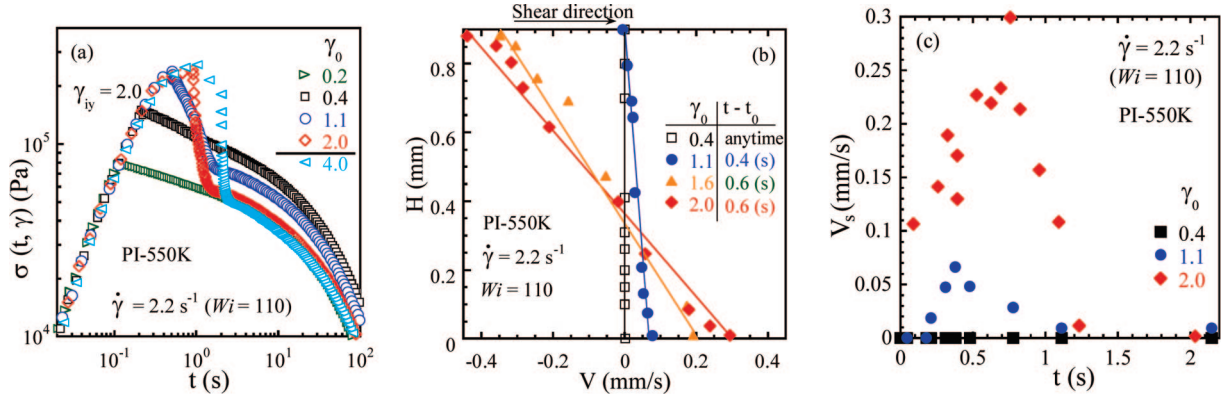

Figure 7. (a) Shear stress growth and relaxation upon and after a series of discretely applied step strains for PI550K melt involving $Wi = 110$. (b) PTV observations of maximum recoil-like motions after different amounts of step strain, where $t_0 = \gamma_0/\dot{\gamma}$ denotes the moment of shear cessation. The squares show that quiescence prevails at small strains. The other three symbols describe the recoil motions at the different moments after shear cessation. (c) PTV measurements reveal a finite induction time required for the interface to collapse for $\gamma_0 = 1.1$. Even for $\gamma_0 = 2.0$ where interfacial failure is to begin during continual shear, the interfacial velocity takes a noticeable amount of time to speed up. There is no slip at a step strain of amplitude $\gamma_0 = 0.4$.

filled triangles in Figure 6b,c depict a great deal of sample recoil, as the PI melts take advantage of the interfacial failure that occurred during shear. As a consequence of the elastic recoil, the shear stress was rapidly relieved.

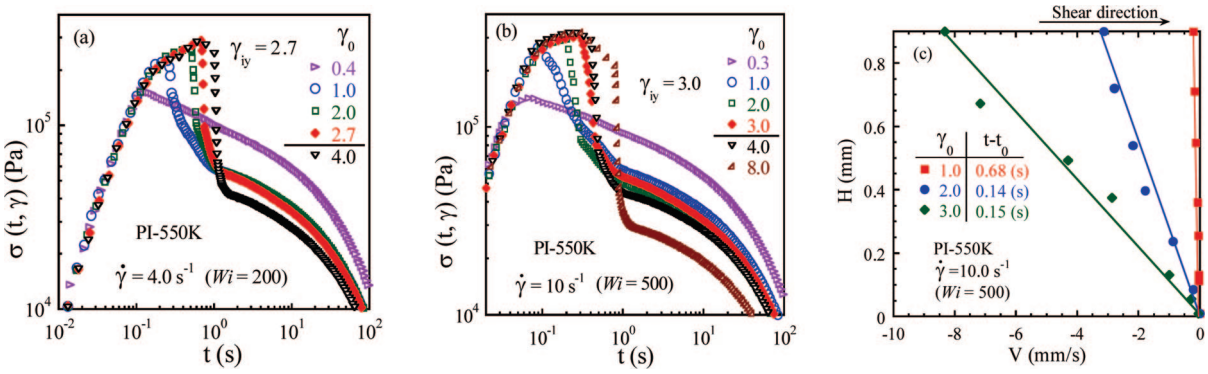

Figure 8. Shear stress growth and relaxation of PI550K upon and after a series of discretely applied step strains of amplitude γ_0 involving (a) $Wi = 200$ and (b) $Wi = 500$. (c) PTV visualization of recoil-like motions after the different amounts of step strain as depicted in (b), where $t_0 = \gamma_0/\dot{\gamma}$ denotes the moment of shear cessation.

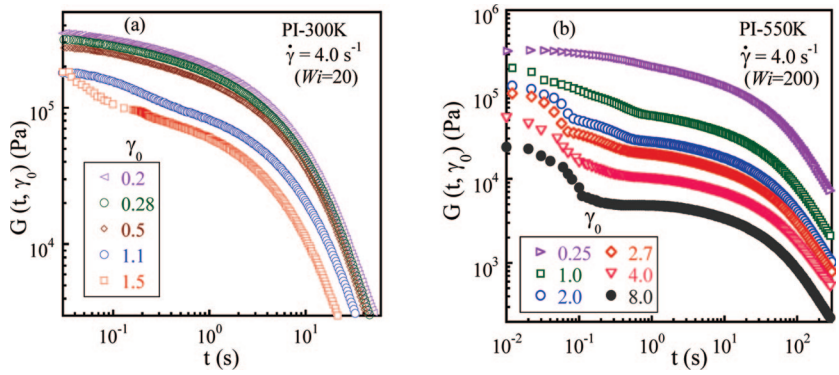

Figure 9. Apparent relaxation modulus $G(t,\gamma_0)$ for (a) PI300K and (b) PI550K melts, respectively.

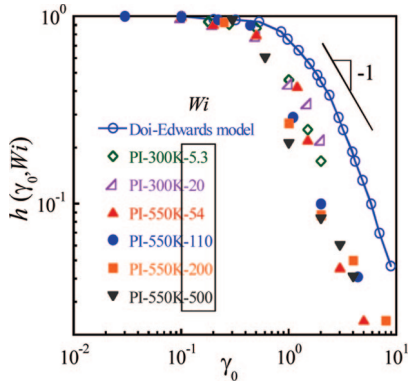

Figure 10. Damping function $h(\gamma_0)$, which conveniently normalizes and summarizes all the stress relaxation measurements in the superimposable domain, decreases with the amplitude γ_0 of step strain more strongly than reciprocally starting at $\gamma_0 \sim 1.0$.

C. Arrested Interfacial Failure after Shear Cessation. Previous studies[30−32] based on step strain experiments typically reported the relaxation dynamics and omitted the data involving the actual startup shear. Our PTV observations allow us to determine when interfacial failure occurs (at γ_{iy}) during startup shear as shown in Figure 6a−c. Such information missing in the literature reveals whether step strain experiment has been properly carried out.

To investigate nonlinear responses after shear cessation, we perform a startup shear up to an amplitude of $\gamma < \gamma_{iy}$, before the shear stress reaches its maximum. In other words, the sudden startup shear is interrupted before interfacial failure is visible by PTV. Figure 7a depicts such interrupted shear tests at a set of discrete strain amplitudes. Apart from the linear responses at low strains of 0.2 and 0.4, Figure 7a shows accelerated stress decline after shear cessation at $\gamma_0 = 1.1$, 2.0, and 4.0. Thanks to *in situ* PTV observations of these step strain tests, we are able to understand why the stress decline occurs.

Figure 7b reveals that the sample would relax quiescently at low strain of 0.4. Upon shear cessation at strains of 1.1, 1.6, and 2.0, however, the PI550K melt is observed to undergo interfacial failure, with the maximum interfacial velocity reaching over 0.4 mm/s, which is about twice as high as the maximum slip velocity $V_{s(max)}$ tabulated in Table 1.

It is interesting to examine this arrested interfacial failure more closely. Figure 7c confirms that for $\gamma_0 = 1.1$ no motion due to interfacial failure is measurable until 0.18 s after the moment t_0 of shear cessation. In other words, the surface velocity on the bottom plate takes a finite amount of time to build up as the sample fights against the elastic restoring force before giving in and losing its adhesion. The delayed interfacial yielding[33] is fully anticipated according to the theoretical understanding offered in section III.B: upon shear cessation, the intermolecular locking force turns off and is unavailable to balance against the elastic retraction force, resulting in chain disentanglement.

V. Conclusion

Wall slip and interfacial yielding are an important characteristic of well-entangled polymers and are prevalent in polymer processing. They also make rheological experiments challenging to perform. Failure to recognize their occurrence has invalidated comparison of many experimental data with theory. In other words, the lack of a better understanding of how and why interfacial yielding takes place during or after shear has caused us to ignore its occurrence. In our new picture, analogous to that for cohesive yielding reported earlier,[23,34] wall slip is nothing but yielding taking place at the polymer/wall interface, and the onset of this interfacial failure occurs at higher strains for a higher applied rate of shear. Analogous to the observation

of internal macroscopic motions after a modest step strain, our particle-tracking velocimetric experiments reveal interfacial failure after shear cessation. This arrested interfacial failure is direct evidence that the elastic retraction force associated with the chain deformation is capable of overcoming interfacial cohesion (i.e., adhesion in abbreviation). Apparently, the elastic retraction force due to a sudden step strain with amplitude $\gamma_0 \sim 1.0$ is sufficient to overcome, upon shear cessation, the entanglement interactions between adsorbed and bulk chains. During shear, as discussed in section III, there is an active component (f_{iml}) of intermolecular interactions that act against the elastic retraction force, postponing interfacial yielding to a higher strain of $\gamma_{iy} > 1.0$. Termination of the applied shear causes the force imbalance to occur before γ_{iy} is reached, leading to the arrested failure.

Acknowledgment. This work is supported, in part, by a small grant for exploratory research (DMR-0603951) and a standard grant (DMR-0821697) from Polymers program of the National Science Foundation.

Appendix. Ultra Strain Softening

The interfacial yielding and failure show additional characteristics when examined at different applied rates of shear. Figure 8a,b along with Figure 7b shows how the onset of interfacial failure shifts to higher strain γ_{iy} at higher rates, increasing from 2.0 to 3.0 as *Wi* increases from 110 to 500. Such an approximate trend of $\gamma_{iy} \sim \dot{\gamma}^{1/3}$ is consistent with the scaling behavior associated with yielding (stress overshoot) in entangled polymer solutions[34] and melts.[35] At the higher strains, Figure 8c shows much stronger recoil motion where the interfacial velocity far exceeds the maximum wall slip velocity $V_{s(max)} \sim 0.2$ mm/s. This implies that cohesive failure (i.e., bulk chain disentanglement) has taken place.

From data such as those in Figures 7a and 8a,b, we can evaluate the "apparent relaxation modulus", bearing in mind that the true meaning of relaxation modulus $G(\gamma_0,t)$ is lost whenever there is macroscopic motion upon shear cessation. Borrowing this inapplicable notion of relaxation modulus $G(\gamma_0,t) = \sigma(\gamma_0,t)/\gamma_0$, we evaluate G to show in Figure 9a,b that severe strain softening occurs at strains beyond unity.

In the literature, it was common to report a damping function and compare experimental data to the Doi−Edwards theory because of the consensus that the Doi−Edwards theory gives the expected stress relaxation behavior in absence of interfacial failure. The damping function $h(\gamma_0)$ is a normalized way to represent the stress relaxation behavior, involving division of $G(\gamma_0, t > t_b)$ by the well-defined relaxation modulus $G_e(t > t_b)$ obtained in the linear response regime. As demonstrated by the experimental data in Figure 9a,b, the representation in terms of h is possible because the relaxation behavior at time $\tau > t > t_b$ is identical at all strains. The PTV observations disclose the significance of t_b: Beyond t_b the sample ceases to recoil, i.e., the interface has repaired itself by this time, allowing the subsequent stress relaxation to occur in the same manner as that due to a small step strain.

Summarizing all the data in Figure 10, we show that due to interfacial failure either during shear or after shear cessation considerable "strain softening" occurs, relative to the Doi−Edwards damping function h_{DE}. It is important to point out that these data as well as the Doi−Edwards curve amounts to[36] revealing a lower shear stress $\sigma(\gamma_0, t > t_b) \sim \gamma_0 h(\gamma_0)$ at higher strains; i.e., h decreases faster than $1/\gamma_0$. Our PTV observations reveal that this trend is possible because interfacial failure is more severe at higher strains, allowing the sample to recoil more strongly and relax shear stress more quickly. The ultra strain softening observed 25 years ago[31] perhaps had the same origin: interfacial failure.

References and Notes

(1) De Gennes, P. G. *C. R. Acad. Sci.* **1979**, *219*, 288B.
(2) Brochard, F.; de Gennes, P. G. *Langmuir* **1992**, *8*, 3033.
(3) Ajdari, A.; Brochard-Wyart, F.; de Gennes, P. G.; Leibler, L.; Viovy, J. L.; Rubinstein, M. *Physica A* **1994**, *104*, 17.
(4) Brochard-Wyart, F.; Gay, C.; de Gennes, P.-G. *Macromolecules* **1996**, *29*, 377.
(5) Mhetar, V.; Archer, L. A. *Macromolecules* **1998**, *31*, 6639.
(6) Yarin, A. L.; Graham, M. D. *J. Rheol.* **1998**, *42*, 1491.
(7) Joshi, Y. M.; Lele, A. K. *J. Rheol.* **1998**, *46*, 427.
(8) Joshi, Y. M.; Lele, A. K.; Mashelkar, R. A. *Macromolecules* **2001**, *10*, 3412.
(9) Vinogradov, G. V.; Malkin, A. Y.; Yanovskii, Y. G.; Borisenkova, E. K.; Yarlykov, B. V.; Berezhnaya, G. V. *J. Polym. Sci., Part A* **1972**, *2*, 1061.
(10) Yang, X. P.; Wang, S. Q.; Halasa, A.; Ishida, H. *Rheol. Acta* **1998**, *37*, 415.
(11) Boukany, P. E.; Wang, S. Q. *J. Rheol.* **2006**, *50*, 641. where Figure 1b illustrates how wall slip is depicted in terms of either slip velocity V_s or extrapolation length b.
(12) Kalika, D. S.; Denn, M. M. *J. Rheol.* **1987**, *31*, 815.
(13) Hatzikiriakos, S. G.; Dealy, J. M. *J. Rheol.* **1991**, *35*, 197.
(14) Hatzikiriakos, S. G.; Dealy, J. M. *J. Rheol.* **1992**, *36*, 845.
(15) Koran, F.; Dealy, J. M. *J. Rheol.* **1999**, *43*, 1291.
(16) Durliat, E.; Hervet, H.; Leger, L. *Europhys. Lett.* **1997**, *38*, 383.
(17) Leger, L.; Hervet, H.; Massey, G.; Durliat, E. *J. Phys.: Condens. Matter* **1997**, *9*, 7719.
(18) Leger, L.; Hervet, H.; Charitat, T.; Koustos, V. *Adv. Colloid Interface Sci.* **2001**, *94*, 39.
(19) Mhetar, V.; Archer, L. A. *Macromolecules* **1998**, *31*, 8607.
(20) Dao, T. T.; Archer, L. A. *Langmuir* **2002**, *18*, 2616.
(21) Wang, S. Q. *Adv. Polym. Sci.* **1999**, *138*, 227.
(22) Wang, S. Q. *Macromol. Mater. Eng. Sci.* **2007**, *129*, 215.
(23) Wang, S. Q.; Ravindranath, S.; Wang, Y. Y.; Boukany, P. *J. Chem. Phys.* **2008**, *127*, 064903.
(24) Wang, Y. Y.; Wang, S. Q. *Macromolecules*, under review (2009). Here we proposed that the intermolecular locking force f_{iml} increases with the local shear rate $\dot{\gamma}$ and decreases with molecular orientation or deformation γ that can be estimated based on the affine deformation approximation of $\gamma = \dot{\gamma}t$.
(25) Boukany, P. E.; Wang, S. Q. *J. Rheol.* **2007**, *51*, 217.
(26) Doi, M.; Edwards, S. F. *The Theory of Polymer Dynamics*, 2nd ed.; Clarendon Press: Oxford, 1988.
(27) Fetters, L. J.; Lohse, D. J.; Richter, D.; Witten, T. A.; Zirkel, A. *Macromolecules* **1994**, *27*, 4639.
(28) Wang, S. F.; Wang, S. Q.; Halasa, A.; Hsu, W.-L. *Macromolecules* **2003**, *36*, 5355.
(29) Boukany, P. E.; Wang, S. Q. *Macromolecules*, to be submitted (2009).
(30) Osaki, K.; Nishizawa, K.; Kurata, M. *Macromolecules* **1982**, *15*, 1068.
(31) Vrentas, C. M.; Graessley, W. W. *J. Rheol.* **1982**, *26*, 359.
(32) Sanchez-Reyes, J.; Archer, L. A. *Macromolecules* **2002**, *35*, 5194.
(33) "Delayed slip" has been reported once before by: Archer, L. A.; Larson, R. G. *J. Rheol.* **1995**, *39*, 519. However, its physical origin has been elusive in the past.
(34) Ravindranath, S.; Wang, S. Q. *J. Rheol.* **2008**, *52*, 681.
(35) Boukany, P. E.; Wang, S. Q. *J. Rheol.* **2009**, in press.
(36) Ravindranath, S.; Wang, S. Q. *Macromolecules* **2007**, *40*, 8031.

MA802644R